

and E. Burstein, *ibid.*, p. 739.

⁵We used optical constants of GaAs from the following authors: H. R. Philipp and H. Ehrenreich, *Phys. Rev.* **129**, 1550 (1963); M. D. Sturge, *Phys. Rev.* **127**, 768 (1962).

⁶R. Loudon, *Advan. Phys.* **13**, 423 (1964).

⁷Equation (1) is equivalent to the zeroes of the longitudinal dielectric function $\epsilon_T(q, \omega)$. This expression is also obtained by determining the poles of the phonon propagator: See for instance G. Mahan, in *Polarons in Ionic Crystals and Polar Semiconductors*, edited by J. T. Devreese (North-Holland, Amsterdam, 1972), p. 553.

⁸J. Lindhard, *Kgl. Dan. Vidensk. Selsk., Mat.-Fys. Medd.* **28**, No. 8 (1954); see also D. Pines, *Elementary Excitations in Solid* (Benjamin, New York, 1964), p. 143.

⁹ $L_-(q)$ mode was discussed by Cowley and Dolling in order to explain the dispersion curves of the LO modes in PbTe with electron density $(1-3) \times 10^{19} \text{ cm}^{-3}$; R. A. Cowley and G. Dolling, *Phys. Rev. Lett.* **14**, 549 (1965). The data had been obtained by Cochran from neutron-

scattering experiments; W. Cochran, *Phys. Lett.* **13**, 193 (1964). It should be noted that they used a static dielectric constant, $\epsilon_e(q, 0)$ in Eq. (1), with a good approximation; such is not true in our GaAs system. Moreover, neutron scattering is not useful in our system, since the wave-number resolution is more than a factor of 10 inferior to that in the present experiment in spite of the evanescent light.

¹⁰M. Cardona, *Phys. Rev.* **121**, 752 (1961).

¹¹D. L. Mills, A. A. Maradudin, and E. Burstein, *Phys. Rev. Lett.* **21**, 1178 (1968); M. Inoue and T. Moriya, *J. Phys. Soc. Jpn.* **29**, 117 (1970).

¹²C. A. Mead and W. G. Spitzer, *Phys. Rev.* **134**, A713 (1964).

¹³D. J. Evans, S. Ushioda, and J. D. McMullen, *Phys. Rev. Lett.* **31**, 369 (1973).

¹⁴R. Tsu, H. Kawamura, and L. Esaki, *Solid State Commun.* **15**, 321 (1974).

¹⁵Note that very recently Yu and Shen also used a similar method to study dispersive Raman methods in Cu_2O : P. Y. Yu and Y. R. Shen, *Phys. Rev. Lett.* **32**, 939 (1974).

Pentapyridinium 18-Silver Iodide, a "Two-Dimensional" Solid Electrolyte*

S. Geller and P. M. Skarstad

Department of Electrical Engineering, University of Colorado, Boulder, Colorado 80302

(Received 2 July 1974)

The new solid electrolyte pentapyridinium 18-silver iodide, $(\text{C}_5\text{H}_5\text{NH})_5\text{Ag}_{18}\text{I}_{23}$, effectively allows the current-carrying Ag^+ ions to move in only two dimensions. Comparison with the other solid electrolyte in the $\text{C}_5\text{H}_5\text{NH}-\text{AgI}$ system, namely $(\text{C}_5\text{H}_5\text{NH})\text{Ag}_5\text{I}_6$, demonstrates that three-dimensionally interconnecting diffusion pathways are more favorable to high conductivity.

We report a new solid electrolyte in the pyridinium-iodide-silver-iodide system in which the current carriers (the Ag^+ ions) are forced to stay within layers perpendicular to the hexagonal c axis of the crystal. There are no paths by which the Ag^+ ions can move between these layers, which are separated by layers of (effectively) $[(\text{C}_5\text{H}_5\text{NH})_3\text{I}]^{2+}$ ions. As a result, the average conductivity of the material is low. This is further corroboration of the thesis that three-dimensional connectivity is probably best for highly conducting solid electrolytes.

There are two compounds in the system of pyridinium iodide and silver iodide (PyI-AgI) which are now known to be solid electrolytes. The relation of the conductivity-versus-temperature behavior to the crystal structure and Ag^+ -ion site distribution of $(\text{C}_5\text{H}_5\text{NH})\text{Ag}_5\text{I}_6$ has been previously reported.¹ $(\text{C}_5\text{H}_5\text{NH})\text{Ag}_5\text{I}_6$ is a three-dimensional solid electrolyte and has a room-temperature

average conductivity of $0.077 (\Omega \text{ cm})^{-1}$, almost an order of magnitude higher than that, $0.008 (\Omega \text{ cm})^{-1}$, of $(\text{C}_5\text{H}_5\text{NH})_5\text{Ag}_{18}\text{I}_{23}$, the two-dimensional solid electrolyte (Fig. 1).

Figure 1(a) is a top view of the iodide-ion arrangement in the crystal (space group, $P\bar{6}2m$; $a = 13.62$, $c = 12.58 \text{ \AA}$, $Z = 1$) of $\text{Py}_5\text{Ag}_{18}\text{I}_{23}$.² The paths for the Ag^+ ions are shown in Fig. 1(b) and result from the sharing of faces of iodide tetrahedra. Figure 1(c), which is a side view of the structure, illustrates clearly how the Ag^+ ions are constrained to move between layers of (effectively) $[(\text{C}_5\text{H}_5\text{NH})_3\text{I}]^{2+}$ ions. There are no paths for Ag^+ -ion diffusion crossing these layers [see also Fig. 1(d)]. Two-fifths of the $(\text{C}_5\text{H}_5\text{NH})^+$ ions are stacked along the hexagonal c axes.

For comparison, a top view of PyAg_5I_6 is shown in Fig. 2. This crystal (space group, $P6/mcc$, $a = 12.03$, $c = 7.43 \text{ \AA}$, $Z = 2$) has three-dimensional pathways for Ag^+ -ion diffusion. (These pathways

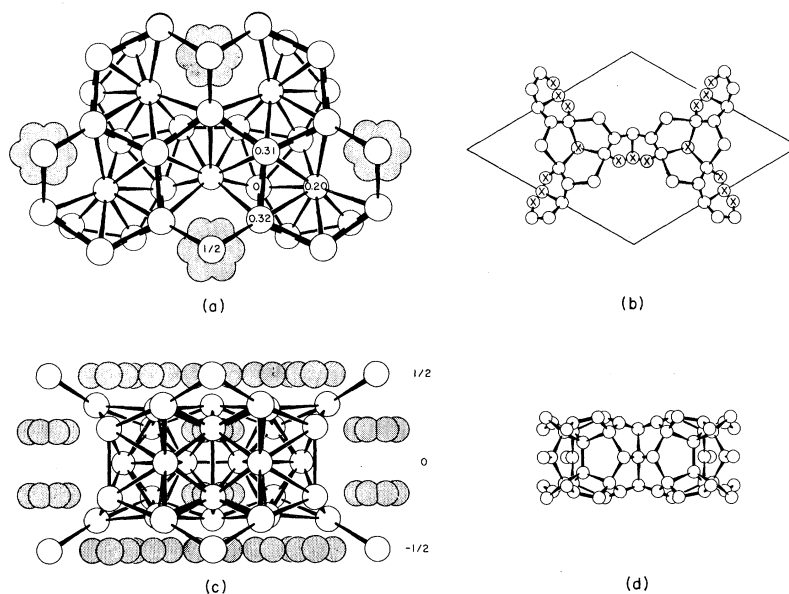


FIG. 1. (a) Top view of iodide-ion arrangement in $\text{Py}_5\text{Ag}_{18}\text{I}_{23}$. The pyridinium ions (stippled) on the hexagonal axes are also shown. (b) Top view of Ag^+ -ion paths in $\text{Py}_5\text{Ag}_{18}\text{I}_{23}$. The equilibrium Ag^+ -ion sites (located at or near iodide tetrahedra centers) are shown. A cross indicates a connection between upper and lower halves of the Ag^+ path network within the conducting layer. See also (d). (c) Side view of the iodide arrangement in $\text{Py}_5\text{Ag}_{18}\text{I}_{23}$. The pyridinium ions (stippled) in the $\pm \frac{1}{2}c$ levels of the unit cell are shown. These together with the I^- ions at $\pm (0, 0, \frac{1}{2})$ block movement of Ag^+ ions in the c -axis direction. (d) Side view of the Ag^+ -ion paths in $\text{Py}_5\text{Ag}_{18}\text{I}_{23}$.

are therefore more difficult to visualize.) The $(\text{C}_5\text{H}_5\text{NH})^+$ ions are *all* stacked along the hexagonal c axes. Details on pathways in PyAg_5I_6 have already been given elsewhere.¹

PyAg_5I_6 has a transition at 50°C from a region of low disorder to one of high disorder.¹ In the higher-temperature region, h_m , the enthalpy of activation of motion, is 0.21 eV. This is the value of h_m found between room temperature and 100°C for $\text{Py}_5\text{Ag}_{18}\text{I}_{23}$.² At 55°C , the (average) specific conductivities of PyAg_5I_6 and $\text{Py}_5\text{Ag}_{18}\text{I}_{23}$ are 0.29 and $0.015 (\Omega \text{ cm})^{-1}$, respectively, differing by a factor of 19.

A strict comparison of conductivities cannot be made [except for isostructural compounds, e.g., RbAg_4I_5 ,^{3,4} KAg_4I_5 , and $(\text{NH}_4)\text{Ag}_4\text{I}_5$, in which case nothing really new is learned] because the crystal structures are so different. $\text{Py}_5\text{Ag}_{18}\text{I}_{23}$ has seven crystallographically nonequivalent sets of equilibrium sites for the Ag^+ ions, PyAg_5I_6 only three; the former contains only face-sharing tetrahedra, the latter both octahedra and tetrahedra sharing faces with each other and among themselves but in a very different manner from that in $\text{Py}_5\text{Ag}_{18}\text{I}_{23}$. The respective Ag^+ -ion concentrations⁵ (0.89 and 1.07) $\times 10^{22} \text{ cm}^{-3}$ are quite different as are the Ag^+ -ion equilibrium-site concentrations⁶ (2.72 and 3.65) $\times 10^{22} \text{ cm}^{-3}$. On

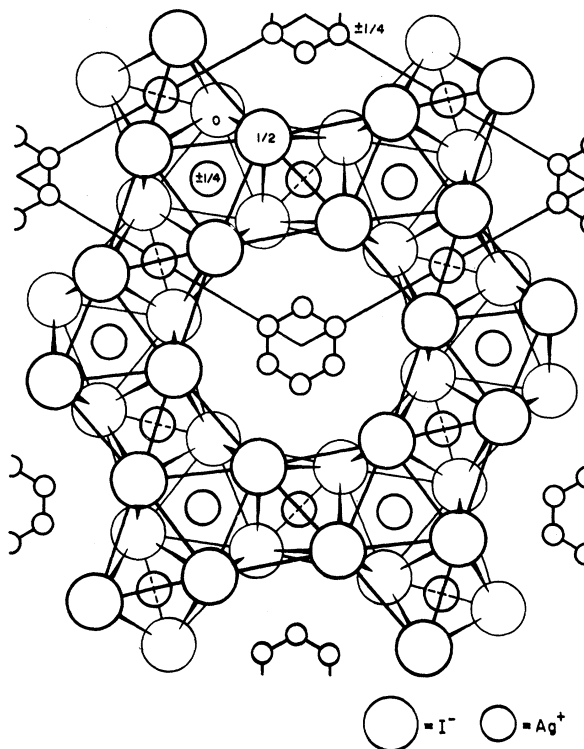


FIG. 2. Top view of the crystal structure in PyAg_5I_6 at -30°C . As temperature increases, Ag^+ ions increasingly move into the tetrahedra which are empty in this figure. (From Ref. 1.)

the other hand, the two-dimensional solid electrolyte *implies* lower concentrations of Ag^+ ions and equilibrium sites, simply because it must contain ions or atoms which *block* the motions of the current carriers in one of the crystal dimensions.

It can readily be shown² that the total volume of the crystal occupied by the pathways themselves is lower for the two-dimensional solid electrolyte than for any of the three-dimensional solid electrolytes, $(\text{C}_5\text{H}_5\text{NH})\text{Ag}_5\text{I}_5$, RbAg_4I_5 , $[(\text{CH}_3)_4\text{N}]_2\text{Ag}_{13}\text{I}_{15}$, whose structures^{1,4,7} have been determined. Both the carrier concentrations and the conductivities of each of these three-dimensional solid electrolytes are higher than those of $\text{Py}_5\text{Ag}_{18}\text{I}_{23}$. This implies that those three-dimensional solid electrolytes that have lower conductivities than $\text{Py}_5\text{Ag}_{18}\text{I}_{23}$ will have lower carrier concentrations, lower volume fractions occupied by the conducting pathways, and probably more complex pathways.

Sodium β -alumina, a material which is also a two-dimensional solid electrolyte, does not attain a high conductivity until relatively high temperature; at 100°C, for example,⁸ σ_1 is $0.077 (\Omega \text{ cm})^{-1}$ [note that Whittingham and Huggins⁹ report $\sigma_1 = 0.0382 (\Omega \text{ cm}^{-1})$]; for $\text{Py}_5\text{Ag}_{18}\text{I}_{23}$ it is¹⁰ $0.05 (\Omega \text{ cm})^{-1}$.

The results and comparisons given here demonstrate the high probability that three-dimensional pathways for diffusion of the ionic current carriers are most favorable for high-conductivity solid electrolytes. It is to be emphasized that simplicity and numerous interconnections of these pathways enhance the conductivity. {For example, compare the crystal structures of RbAg_4I_5 ⁴

with those of $[(\text{CH}_3)_4\text{N}]_2\text{Ag}_{13}\text{I}_{15}$ ⁹ and of the two compounds of pyridinium. }

Crystals of $\text{Py}_5\text{Ag}_{18}\text{I}_{23}$ were grown by G. P. Espinosa. Measurements of average specific conductivity were made by S. A. Wilber.

*Work supported by the National Science Foundation under Grant No. GH37102.

¹S. Geller and B. B. Owens, *J. Phys. Chem. Solids* **33**, 1241 (1972); S. Geller, *Science* **176**, 1016 (1972).

²Details on the crystal-structure determination and measurements of conductivity and further discussion thereof are to be published.

³B. B. Owens and G. R. Argue, *Science* **157**, 308 (1967).

⁴S. Geller, *Science* **157**, 316 (1967).

⁵It should be emphasized that in $\text{Py}_5\text{Ag}_{18}\text{I}_{23}$, as well as in all other AgI-based solid electrolytes for which accurate determinations have been made, the equilibrium distribution of Ag^+ ions over crystallographically nonequivalent sites is markedly nonuniform.

⁶These are the estimated values at 55°C. The lattice constants of $\text{Py}_5\text{Ag}_{18}\text{I}_{23}$ have not been measured at this temperature, but were assumed to increase by the same factor as those of PyAg_5I_6 which have been measured (Ref. 1). The 55°C concentrations are actually only about 1% lower than the room-temperature values.

⁷S. Geller and M. D. Lind, *J. Chem. Phys.* **52**, 5854 (1970).

⁸A. Imai and M. Harata, *J. Electrochem. Soc.* **117**, 117 (1970). For a review, see J. T. Kummer, in *Progress in Solid State Chemistry*, edited by H. Reiss and J. O. McCaldin (Pergamon, Oxford, England, 1972), Vol. 7, pp. 141-176.

⁹M. S. Whittingham and R. A. Huggins, *J. Chem. Phys.* **54**, 414 (1971).

¹⁰Only $\langle \sigma \rangle$ of $\text{Py}_5\text{Ag}_{18}\text{I}_{23}$ was measured, from which $\sigma_1 = 1.5 \langle \sigma \rangle$.

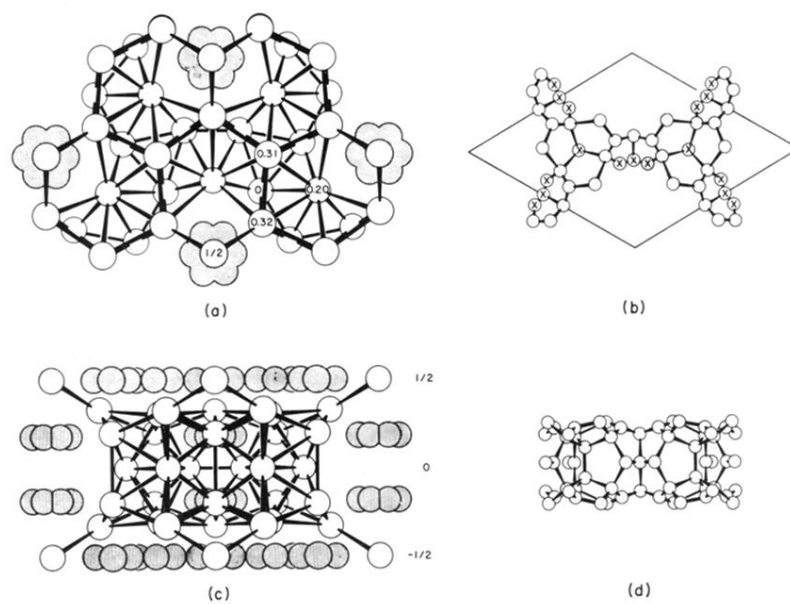


FIG. 1. (a) Top view of iodide-ion arrangement in $\text{Py}_5\text{Ag}_{18}\text{I}_{23}$. The pyridinium ions (stippled) on the hexagonal axes are also shown. (b) Top view of Ag^+ -ion paths in $\text{Py}_5\text{Ag}_{18}\text{I}_{23}$. The equilibrium Ag^+ -ion sites (located at or near iodide tetrahedra centers) are shown. A cross indicates a connection between upper and lower halves of the Ag^+ path network within the conducting layer. See also (d). (c) Side view of the iodide arrangement in $\text{Py}_5\text{Ag}_{18}\text{I}_{23}$. The pyridinium ions (stippled) in the $\pm \frac{1}{2}c$ levels of the unit cell are shown. These together with the I^- ions at $\pm (0, 0, \frac{1}{2})$ block movement of Ag^+ ions in the c -axis direction. (d) Side view of the Ag^+ -ion paths in $\text{Py}_5\text{Ag}_{18}\text{I}_{23}$.